

PAPER • OPEN ACCESS

Removal of Carcinogenic Dyes Congo red (CR) and Bismarck brown Y (BBY) by Adsorption onto Reusable Hydrogels Derived from Acrylamide

To cite this article: Huda S Al-Niaem *et al* 2021 *J. Phys.: Conf. Ser.* **2063** 012011

View the [article online](#) for updates and enhancements.

You may also like

- [Synthesis of polyacetone acrylamide and detection of amine benzene](#)
Wenting Song and Nanjie Mei
- [Sodium Chloride Inhibits Acrylamide Formation During Deep Fat Frying Of Plantain](#)
J.J Omini, O.E Omotosho and O.D Akinyomi
- [Preparation of hemoglobin-modified boron-doped diamond for acrylamide biosensors](#)
K Umam, E Saepudin and T A Ivandini



The Electrochemical Society
Advancing solid state & electrochemical science & technology

241st ECS Meeting

May 29 – June 2, 2022 Vancouver • BC • Canada

Abstract submission deadline: Dec 3, 2021

Connect. Engage. Champion. Empower. Accelerate.
We move science forward



Submit your abstract



Removal of Carcinogenic Dyes Congo red (CR) and Bismarck brown Y (BBY) by Adsorption onto Reusable Hydrogels Derived from Acrylamide

Huda S Al-Niaem¹, *, Ali A Abdulwahid¹ and Whidad S Hanoosh¹

¹Chemistry Department, College of Science, the University of Basrah, Garmat Ali, 61004 Basrah, Iraq

*hudaalniaem@gmail.com

Abstract. Hydrogels of acrylamide (AM), acrylamide\ 2-acrylamido-2-methyl-1-propane sulphonic acid (AMS), and acrylamide\ 2-acrylamido-2-methyl-1-propane sulphonic acid\graphene oxide (AMSGO) were prepared as adsorbents to remove carcinogenic dyes Congo red (CR) and Bismarck brown Y (BBY) from aqueous solutions. Hydrogels were characterized using FSEM and XRD analyses. For both dyes, the synthesized hydrogels demonstrated high adsorption capability at near-neutral pH. Experimental adsorption data were analyzed using the Langmuir and Freundlich isotherm models. It was found that the Langmuir model was more suitable for the experimental data. Kinetic studies found that the pseudo-second-order model demonstrated the best fitting to the experimental data. In addition, thermodynamic studies suggest that the adsorption process was spontaneous and endothermic. The prepared hydrogels were regenerated and reused in four consecutive cycles and it could be applied to remove anionic dyes from aqueous solutions as an effective adsorbent.

1. Introduction

Water is a vital component of both the natural ecosystem and human life. If there is any disturbance in the physicochemical characteristics of water would adversely affect both [1]. Water pollution is the contamination of water by an excess amount of a substance that can cause harm to human beings and/or the ecosystem. It's level subject to pollutant's abundance, pollutant's ecological impact, and water use [2][3]. If these wastewaters are discharged without treatment, they will cause serious damage to the environment [4].

Among water pollutants, dyes (even at very low concentrations) are one of the most dangerous contaminants due to the rapid development of industries. Synthetic materials like plastics, printing, textile, paper, pharmaceuticals, leather, rubber, and paints industries are the main sources of synthetic dye pollution [5]. Azo dyes are the most used dyes, due to their diversity and chemical stability and accounting for more than 60-70% of all dyes [6]. Out of several dyes, Congo red (CR) is a benzidine-based anionic diazo dye [7], possesses mutagenic and carcinogenic properties, and is toxic to human health [8] and harmful to aquatic life [9][10]. Likewise, Bismarck Brown Y (BBY) a cationic diazo dye [11]. Which produced many toxic aromatic amines in water [12].

It is necessary to eliminate the dyes from the water system, but azo dyes are not easily removed from the wastewater by traditional physical, chemical, and biological treatment processes, because of their extreme stability [13]. Hence, the adsorption technique becomes one of the preferable choices to purify the wastewater containing dyes [14], due to its high efficiency, economic viability with a low operational cost, simplicity [15], and easy availability of various adsorbents [16].

Hydrogels are one form of effective adsorbent material that is promising [17], because of their three-dimensional network of polymeric chains and hydrophilic nature [18] resulting from the presences of



function such as hydroxyl ($-OH$), amine ($-NH_2$), sulphonic ($-SO_3H$), carboxyl ($-COOH$), and amide ($-CONH_2$) groups [19]. The chemical structures, crosslinking densities, and compositions of the gels and their sizes have been important factors in their adsorption efficiency [20]. Also, due to their effortless handling, biocompatibility, environmentally friendly nature, and their associated reusability for the development of an effective desorption process [21], Polymeric hydrogels are very effective in dye adsorption. Porous hydrogel structure allows the dye solution to diffuse rapidly into the polymeric network and interact with its functional groups [22]. In past years, hydrogels derived from acrylamide (AM) have gained substantial attention for use as support carriers in biomedical engineering and as specific adsorbents. The introduction of the 2-acrylamido-2-methyl-1-propane sulphonic acid (AMPS) as a co-monomer along with AM can convey the pH responsiveness behavior in AM which can lead to and effectively remove the dye from the gel [23]. AMPS is an anionic monomer susceptible to pH, consisting of a highly ionizable sulfonate group where the acidic groups enhanced the polymeric network's hydrophilicity, which further increases the swelling behavior and may be used for the adsorption of dyes, and other organic contaminants [24]. Graphene oxide (GO) has been used in the hydrogel structure to improve the efficiency of adsorption and to enhance its physical properties. Dye adsorption can be improved by using GO due to its high specific surface area [25] and the presence of various oxygen-rich functionalities that allow either be covalent, non-covalent linkages, or a combination of both [26].

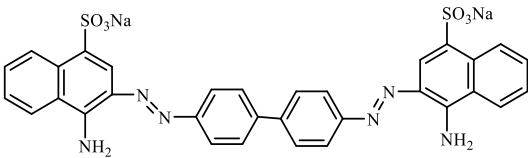
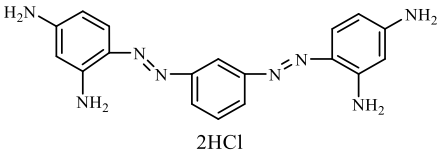
The present study reports an adsorption study of CR and BBY dyes by a hydrogel derived from acrylamide (AM), AM, and AMPS-based hydrogel, and its composite with GO as possible polymeric adsorbent was prepared via free radical polymerization. Here, our interest was to increase the adsorption capacity of AM hydrogels with highly hydrophilic functional groups containing chemical reagents such as AMPS with GO. This hydrogel is used as an adsorbent for the removal of CR and BBY dye from its aqueous solution. Batch adsorption studies are conducted.

2. Materials and Methods

2.1. Materials and measurements

All chemicals used were analytical reagent grades. They were used without further purification. Congo red (CR) and Bismarck brown Y (BBY) dyes were purchased from Sigma-Aldrich Company. The dye solutions were prepared in distilled water by dissolving accurately weighed dyes. Some characteristics of dyes were given in table 1.

Table 1. Some characteristics of dyes.

Dyes	Molecular Structure	Molar mass ($g \cdot mol^{-1}$)	C.I. Nr.
Congo Red (CR)		696.7	22120
Bismarck Brown Y (BBY)		419.31	21000

2.2. Methods

2.2.1. Preparation of graphene oxide (GO)

Modified Hummers method for synthesis graphene oxide was carried out [27]. This was included dissolving 2.0 g of graphite and 1.0 g of $NaNO_3$ in 46.0 ml of concentrated H_2SO_4 under an ice bath.

After about 15 min of stirring, 6.0 g of KMnO_4 was gradually added to the suspension by stirring as slowly as possible to control the reaction temperature below $20\text{ }^\circ\text{C}$. The suspension was stirred for two hours and then kept for 30 minutes at $35\text{ }^\circ\text{C}$. 100.0 mL of deionized water was slowly poured into the suspension, allowing the temperature to rise steadily and maintaining the temperature below $98\text{ }^\circ\text{C}$. After 15 min., the suspension was further diluted with warm deionized water to approximately 280.0 ml. 20.0 mL H_2O_2 (30%) was added to remove the residual KMnO_4 and MnO_2 to change the color into luminous yellow. Then, the suspension was filtered and washed until no sulfates were found and the pH of the filtrate was changed to 7 percent aqueous HCl aqueous solution and deionized water, respectively. Graphene oxide GO was dried under vacuum at $50\text{ }^\circ\text{C}$.

2.2.2. Preparation of Acrylamide Hydrogel (AM)

A 1.0 g of Acrylamide (Am), and N, N'-methylene bisacrylamide as crosslinker agent (0.2 g, 20% compared to monomer) were dissolved in 5 mL distilled water with stirring. To this homogeneous solution was then added 1 mL ammonium persulfate (10% W/V) was added as an initiator of the polymerization reaction followed by the addition of 5 drops from N, N, N', N'-tetramethyl ethylene diamine (TMEDA) as an accelerator to the decomposition of initiator with stirring at room temperature for three minutes to complete the polymerization reaction. The resulting hydrogel was dried and washed three times with water to remove any residue of monomer and initiator, filtered, and dried under vacuum at $30\text{ }^\circ\text{C}$.

2.2.3. Preparation of Acrylamide\ 2-Acrylamido-2-methyl-1-propane sulphonic acid (AMS)

A 1.0 g of AMPS was dissolved in 5 mL of distilled water at $35\text{ }^\circ\text{C}$ with stirring then 1.0 g of Am and (0.4 g, 20% compared to monomers) N, N'-methylene bisacrylamide as crosslinker agent in 5 mL distilled water was added with stirring until the solution became homogenous. Then added 1 mL ammonium persulfate (10% W/V) was added as an initiator of the polymerization reaction followed by the addition of 5 drops from N, N, N', N'-tetramethyl ethylene diamine (TMEDA) as an accelerator to the decomposition of initiator with stirring at room temperature for three minutes to complete the polymerization reaction. The resulting hydrogel (Scheme 2.5) was dried and washed three times with water to remove any residue of monomer and initiator, filtered, and dried under vacuum at $30\text{ }^\circ\text{C}$.

2.2.4. Preparation of Acrylamide\ 2-Acrylamido-2-methyl-1-propane sulphonic acid\ Graphene Oxide Composite Hydrogels (AMSGO)

A 1.0 g of AMPS was dissolved in 15 mL of distilled water at $45\text{ }^\circ\text{C}$ with stirring then 1.0 g of Am and (0.4 g, 20% compared to monomers) of N, N'-methylene bisacrylamide as crosslinker agent in 5 mL distilled water were added with stirring until the solution becomes homogenous then 0.1 g GO was added to the monomer's solution. Then added 1 mL ammonium persulfate (10% W/V) was added as an initiator of the polymerization reaction followed by the addition of 5 drops from N, N, N', N'-tetramethyl ethylene diamine (TMEDA) as an accelerator to the decomposition of initiator with stirring at room temperature for three minutes to complete the polymerization reaction. The resulting hydrogel (Figure 1) was dried and washed three times with water to remove any residue of monomer and initiator, filtered, and dried under vacuum at $30\text{ }^\circ\text{C}$.

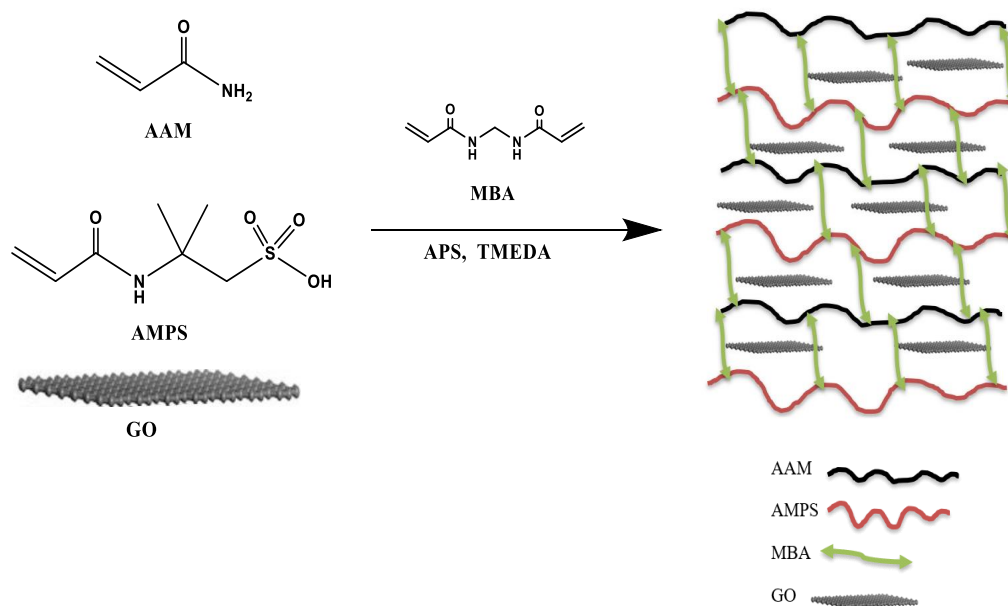


Figure 1. Synthetic routes of preparing AMSGO hydrogel composite.

2.3. Characterization

The morphology of the composite and hydrogels was measured by field-emission scanning electron microscopy (FE-SEM, Nova NanoSEM 450, FEI, USA). The patterns of X-ray diffraction (XRD) were obtained using a Rigaku X-ray Powder Diffractometer (Japan) at a scanning speed of 2 min^{-1} from 5 to 80° ($\text{Cu K}\alpha$ radiation with a wavelength of 1.5406 \AA). Absorption studies were determined by UV-Vis spectrophotometer (T80+, PG InL., UK) between (200- 800) nm using quartz cuvettes with a path length of 1 cm.

2.4. Preparation of Aqueous Dyes Solutions

For the adsorption experiments, a stock solution containing 2000 mg L^{-1} of CR and BBY dyes was used. A dilution using deionized water was provided with the required concentrations.

2.5. Adsorption experiments

Equilibrium adsorption isotherms were determined using the batch studies. Batch adsorption experiments were conducted in stoppered flasks containing 25.0 mg adsorbents and 100 mL of dye solutions with different concentrations ($100\text{-}2000 \text{ mg L}^{-1}$). The adsorption experiments were performed on a thermostat shaker for a night at room temperature (27°C) at 200 rpm. Then, the hydrogels were filtered off, and the concentration of the remaining dye was determined using a UV-Vis spectroscopy at 494 and 457 nm for CR and BBY, respectively. The effect of adsorption isotherms was studied by carrying out a series of isotherms at different temperatures (27 , 45 , and 65°C) and $\text{pH}=(2\text{-}12)$. After adsorption, the adsorbent was separated from the solution by filtration and the concentration of remaining dyes was measured using UV-Visible Spectrophotometer. Adsorption processes were conducted at optimum conditions applying agitation time (60 , 45 , and 45 min), with a pH of 5.0 for AM, 7 for AMS, and AMSGO of the CR dye, respectively. While agitation time (60 , 30 , and 30 min), with a pH of 5.0 for AM, 6 for AMS, and AMSGO of the BBY dye, respectively.

The amount of the CR and BBY dyes on the prepared adsorbents in the equilibrium (q_e) were calculated from the following equation [28]:

$$q_e = \frac{(C_o - C_e)}{W} V \quad (1)$$

where C_o and C_e (mg L^{-1}) are the initial and equilibrium concentrations, respectively of the dye in solution, V (L) is the volume of dyes solution and W (g) is the weight of a hydrogel, and q_e (mg/g) is the amount of adsorbed dyes per gram of adsorbents (adsorption capacity).

In the study of adsorption kinetics and the calculation of kinetic parameters, enthalpy (ΔH°), entropy (ΔS°) and free energy (ΔG°), experiments were conducted at (25, 45 and 65 °C) with 25.0 mg of hydrogels at 0.1 L of (400.0, 1200.0 and 2000 mg L^{-1}) CR solution for AM, AMS, and AMSGO, respectively. While 25.0 mg of hydrogels in 0.1 L of (300.0, 1200 mg L^{-1}) and 0.2 L of 1000 mg L^{-1} , BBY solution for AM, AMS, and AMSGO, respectively. The maximum adsorption capacity was calculated at the optimum pH by changing the pH of the dye solution from 2.0 to 12.0; the pH of the dye solution was adjusted using 0.10 M HCl or NaOH solution.

Four adsorption/ desorption experiments were performed to desorb the dye from hydrogels under the following criteria: using the same adsorbents, maximum adsorption of dye conducted the optimum agitation time and the pH-value for each adsorbent in this work. The desorption experiments were carried out by immersing the dye-loaded adsorbent in 100.0 mL of distilled water and the mixture was continuously stirred for 60 min at room temperature, and the desorbed dyes were separated by centrifugation and filtration, then spectrophotometrically determined the concentration of dyes [29]. The efficiency of dye desorption removal (S) was determined by using the following equation[30]:

$$S \% = \frac{C_d \cdot V_d}{q_e \cdot m} \cdot 100 \% \quad (2)$$

3. Results and discussion

3.1. Characterization of GO and prepared hydrogels

3.1.1. Field Emission Scanning Electron Microscopy (FESEM)

The external surface morphology of prepared hydrogels was analyzed by FESEM (Figure 2a-d). The hydrogel micrographs indicate that they have porous structures. From figure 2a, it can be seen that GO shows a layered and wrinkle-like structure which is due to graphite deformation upon the exfoliation process. Also, the surface appears somewhat bristly with edge planes which can enhance the interaction with dye [31]. On the other hand, as demonstrated in figure 2b, The AM hydrogel shown a smooth and neat surface morphology, the porosity was further enhanced with the incorporation of AMPS in AMS hydrogel (Figure 2c). Also, after the addition of GO into the AMS hydrogel, the surface morphology of the AMSGO composite hydrogel becomes rougher and the AMSGO shows an irregular, plat-like structure (Figure 2d). Furthermore, it can be seen that the GO platelets are well distributed as individual platelets in the hydrogel network and no apparent aggregation has been observed.

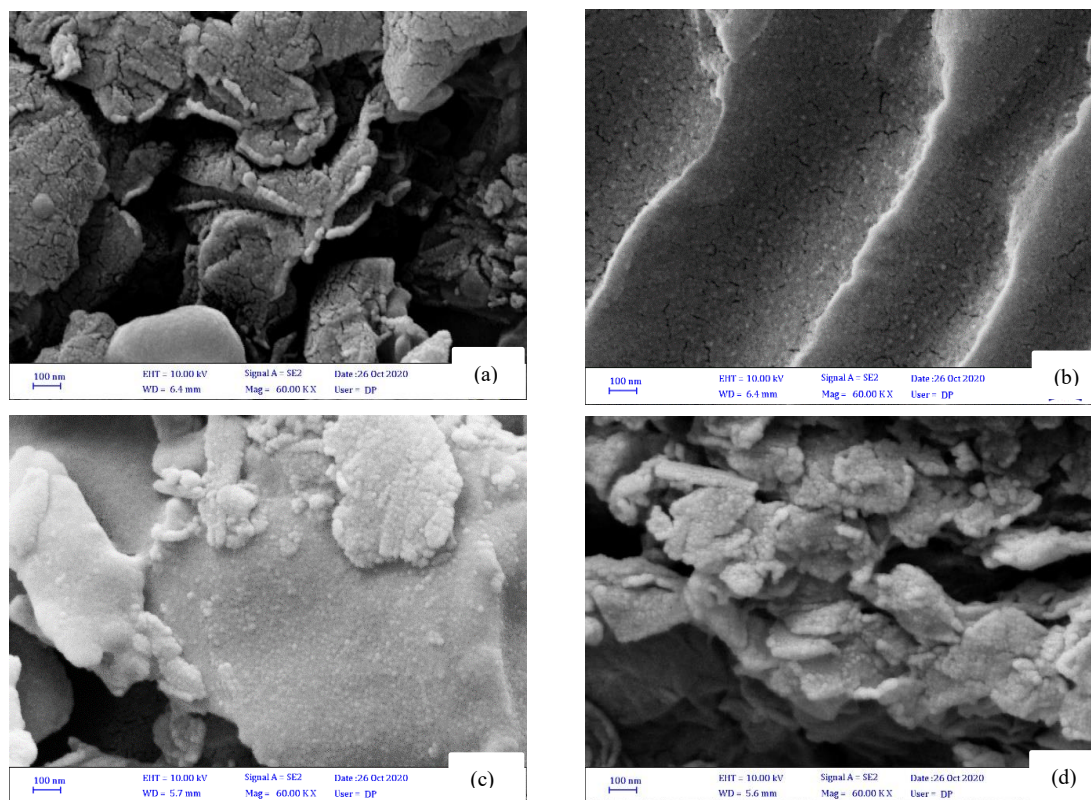


Figure 2. FESEM images of (a) GO, (b) AM, (c) AMS, and (d) AMSGO.

3.1.2. X-ray diffraction (XRD)

The XRD was used as an important method for studying the crystal structure of surface materials. XRD patterns of the GO, AM, AMS, and AMSGO are depicted in figure 3(a-d). As figure 3a for the GO, an intense peak was seen at $2\theta = 10.04^\circ$ was attributed to the diffraction of (001) crystal plane, which was the characteristic peak of GO. The corresponds to an interlayer distance (d) is 0.876 nm, which was attributed to the presence of oxygenated functional groups on GO sheets. After 12^o, The curve progressively tends to be flat, suggesting that the successful oxidation of natural graphite [32]. However, both AM, AMS hydrogels, and AMSGO hydrogel composite exhibit amorphous characters, as shown in figure 2b and c, it also shows a peak at the angle range of (15-30^o), which indicates the amorphous nature of the cross-linked chemical structure of both the hydrogels and its composite [33]. As it was observed in figure 2b and c, a broad non crystalline diffraction peak at ($2\theta = 22.677^\circ$), ($2\theta = 20.783^\circ$), corresponding to an interlayer spacing of ($d = 3.9180\text{A}^\circ$), ($d = 4.2706\text{A}^\circ$), respectively [34]. When comparing the XRD pattern of the GO with the composite hydrogel, clearly noticed the disappearance of the peak at $2\theta = 10.04^\circ$ in the XRD pattern of the AMSGO, and this implied that the GO sheets are completely exfoliated and dispersed evenly in the hydrogel network [32][33].

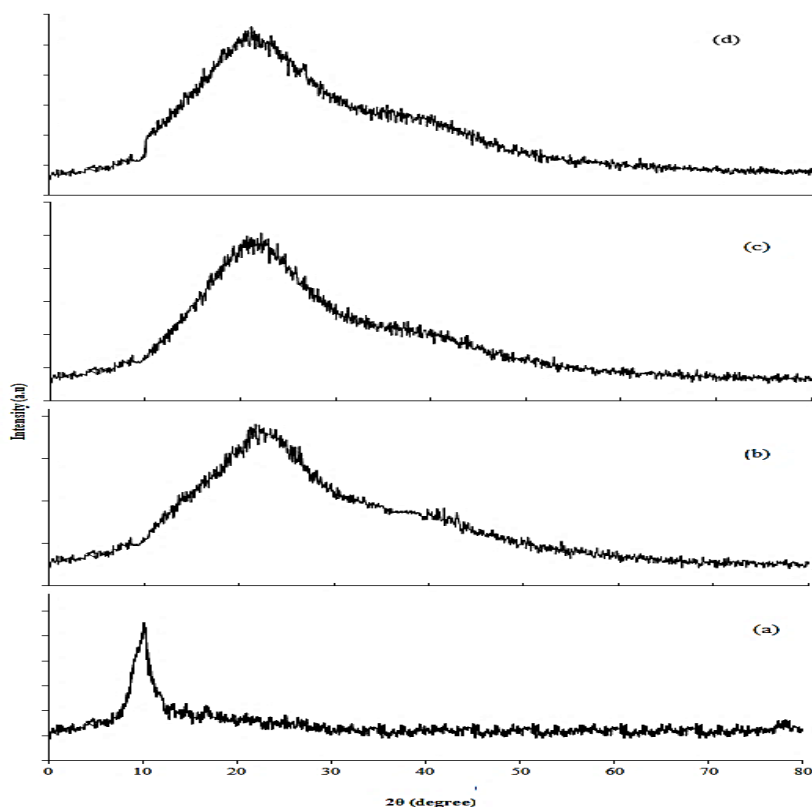


Figure 3. XRD patterns of (a) GO, (b) AM, (c) AMS, and (d) AMSGO.

3.2. Dye Adsorption by the Hydrogel

The CR and BBY dyes adsorption capacity of the prepared hydrogels were examined. The effects of various variables on dye removal were investigated, such as initial dye concentration, pH, time, and temperature, and also other kinetic, isothermal, and thermodynamic parameters.

3.2.1. Effect of pH on Adsorption

The solution's pH value plays an important factor in the adsorption capacity of the dyes onto the hydrogels. The effect of pH on dye's adsorption capacity by prepared hydrogels was investigated at an optimum initial concentration of both CR & BB dyes. The pH was adjusted at the range from 2.0 to 12.0 by 0.1 M NaOH and 0.1 M HCl solution. Figures 3 (a and b) show the pH effect of the adsorption capacities for CR and BBY dyes onto AM, AMS, and AMSGO at 27 °C, respectively. It is apparent that with the increase of pH values, the adsorption capacity of both dyes first increase and then decrease. The maximum adsorption capacity was reached as the pH value approaches 7. With the increasing pH values from 3 to 7, the sulfonic and carboxyl acid groups onto the hydrogels exist as $-\text{COOH}$ and $-\text{SO}_3\text{H}$, which was best suited to the formation of hydrogen bonds between dyes and hydrogels. when pH exceeds 9, adsorption levels of both CR and BBY dyes decrease due to the repulsion of anionic groups on the hydrogel [32].

The results suggest that the optimal pH value was based upon the type of adsorbate used for the adsorption process. Notably, the surface of all hydrogels includes various functional groups, such as sulfonic, carboxylic, and amine groups, these functional groups can ionization by changing the pH values of dye solution.

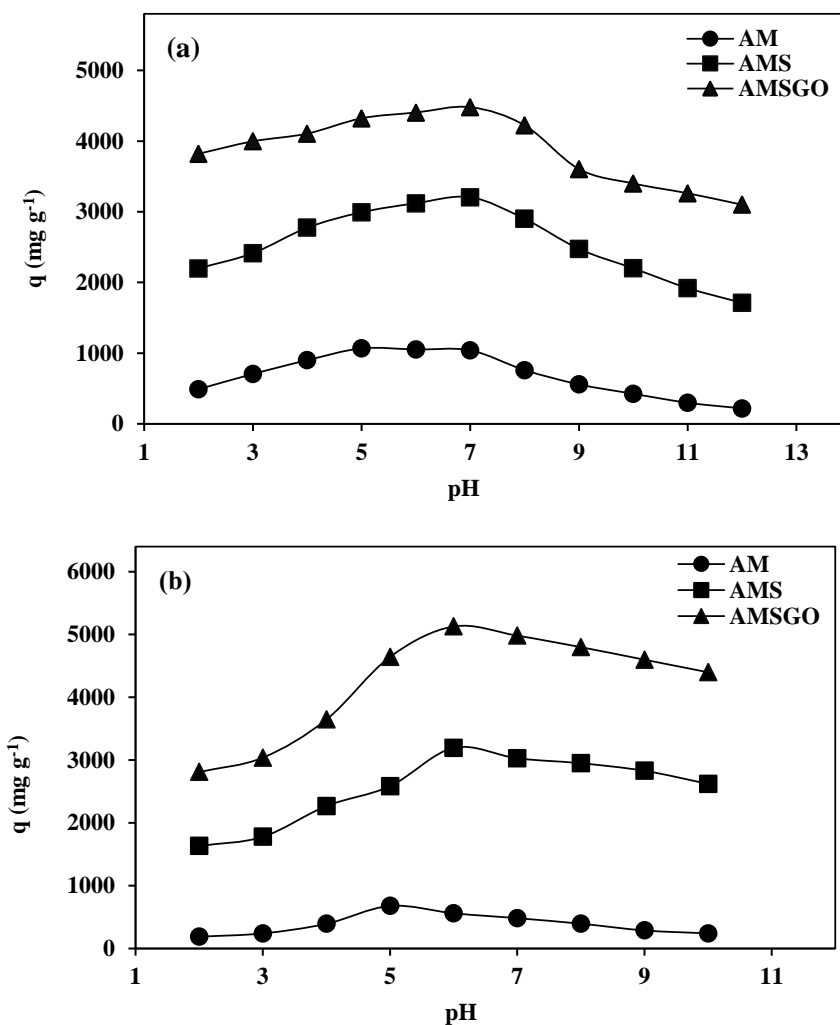


Figure 4. Effect of pH on the adsorption of (a) CR and (b) BBY dyes onto AM, AMG, and AMGGO at 27 °C

3.2.2. Effect of Time and Temperature on Adsorption

The effect of contact time on adsorption of CR and BB dyes onto the prepared hydrogels, at the initial concentration of each adsorbent and optimum pH at different temperatures was investigated. The results are shown in figure 6 and 7, reveals that the adsorption of CR and BBY has rapidly increased from 1 to 60 min, and then the equilibrium is attained within (60-120 min) for AM hydrogel. Also, the behavior of CR dye adsorption by adsorbents AMS and AMSGO as shown in figure 4 has increased rapidly from (1-45 min), and then the equilibrium is achieved within (45-90 min). While figure 5 shows a rapid increase for adsorbents AMS and AMSGO from 1 to 30 min, then the equilibrium is reached within (30-75 min). The trend for both dyes is more or less the same. Initially, the adsorption rate of both dyes was higher because of the availability of a wide number of active sites for adsorption in the hydrogel structure. The adsorption rate gradually decreased due to a reduction in the number of adsorption active sites until equilibrium was achieved. Also, the temperature increases from 25 to 65 °C, the adsorption capacity for all hydrogels are raised. Since the adsorption of CR and BBY were endothermic, this pattern is predicted for the adsorption capability of the adsorbents. Therefore, for all further experiments, the optimal contact times were selected as 60 min for adsorption of CR dye by adsorbent AM and 45 min for both adsorbents AMS and AMSGO. Whereas 60 min for adsorption of BBY dye by AM adsorbents, and 30 min for adsorption of BBY dye by AMS and AMSGO.

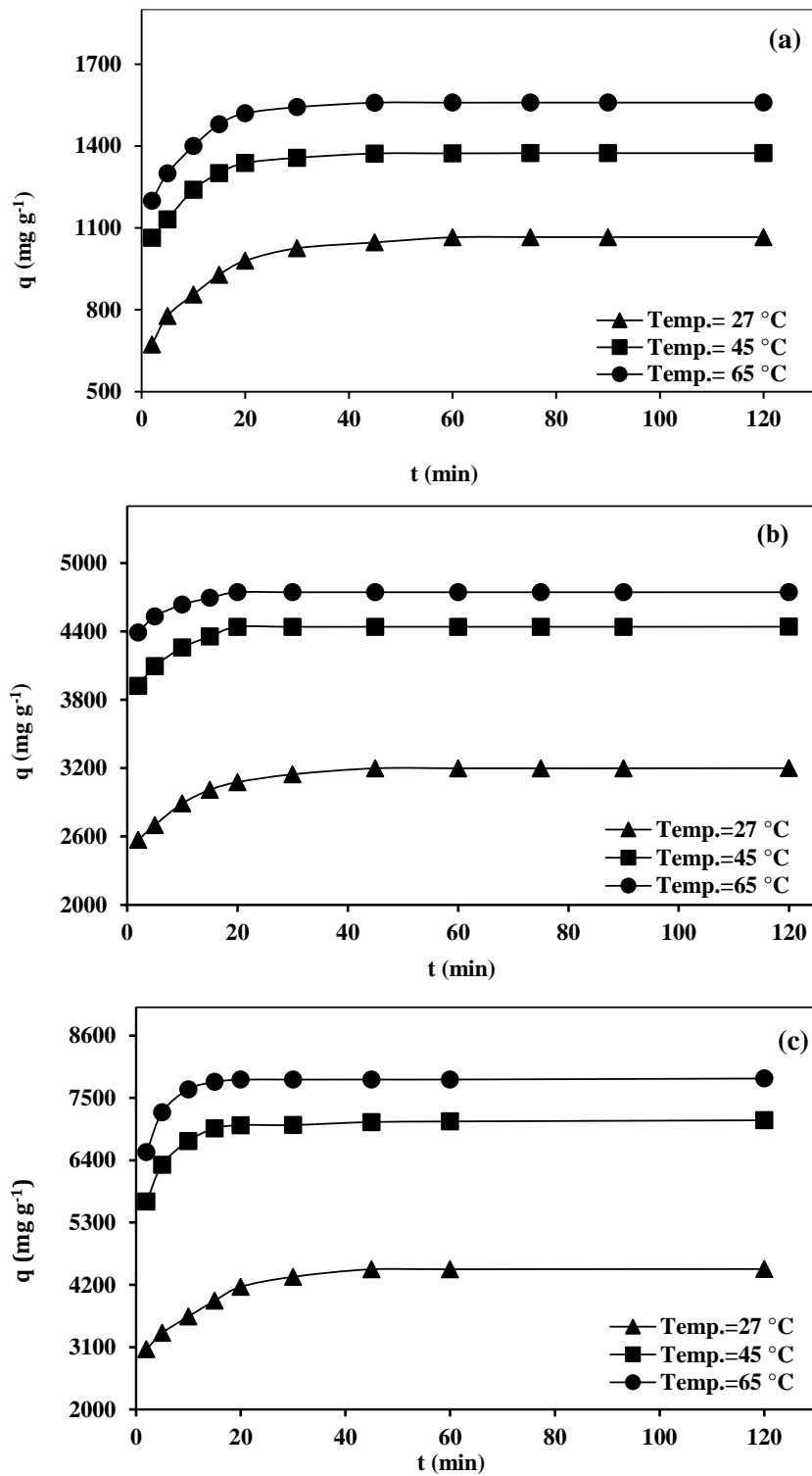


Figure 4. Effect of time on the adsorption of CR dye onto (a) AM, (b) AMG and (c) AMGGO at 27, 45, and 65 °C.

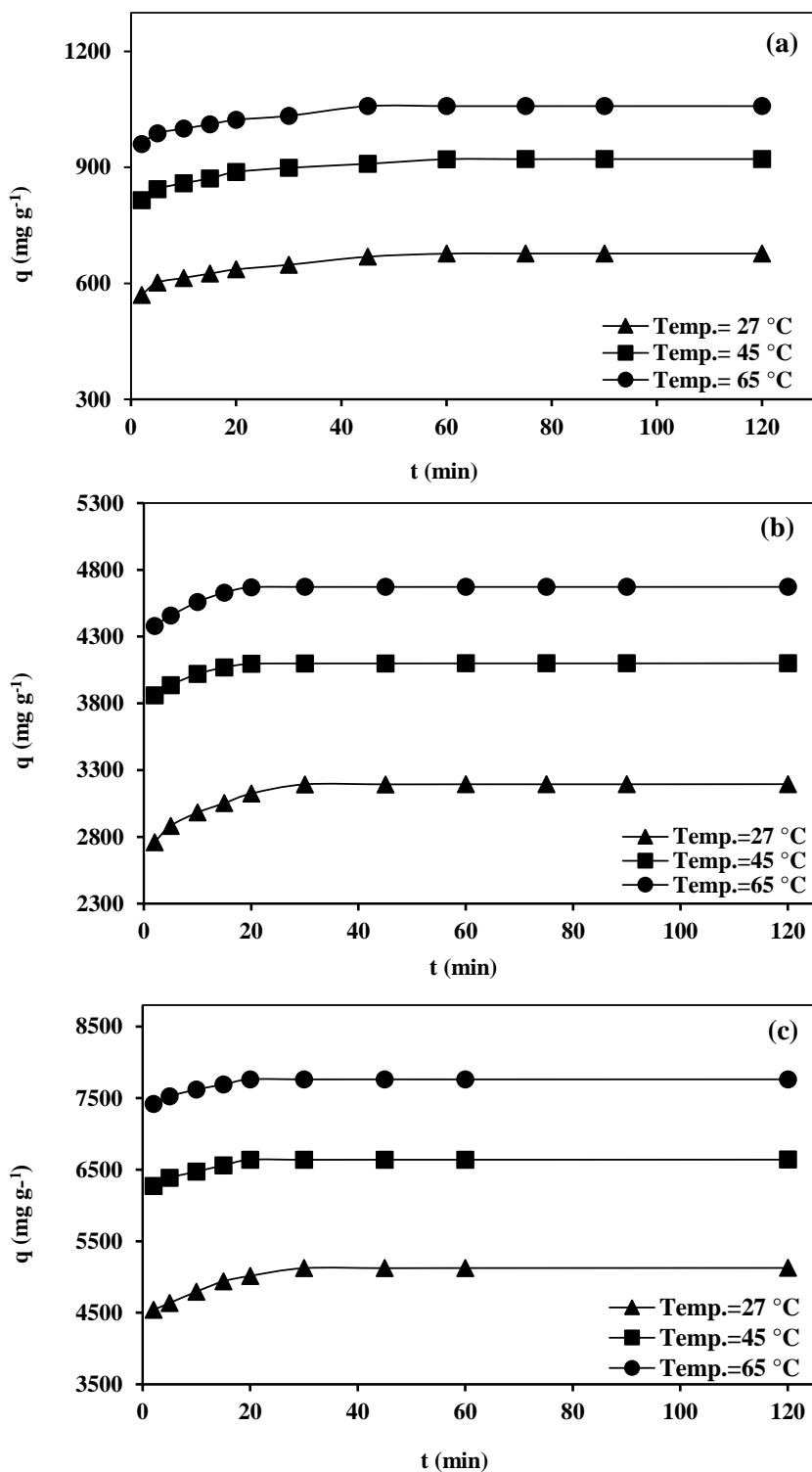


Figure 5. Effect of time on the adsorption of BBY dye onto (a) AM, (b) AMG and (c) AMGGO at 27, 45, and 65 °C.

3.2.3. Adsorption Isotherms

The adsorption isotherms indicate the interaction and equilibrium relationship between adsorbate and adsorbent at a constant temperature [35]. It is necessary to find best-fitting isotherms to describe the adsorption process [36][37]. Adsorption data such as Langmuir and Freundlich isotherms are usually described by adsorption models [38][39]. The Langmuir model describes the mechanism of the adsorption of substances on the surface uniformly [19]. It is based on the homogenous monolayer formation of dyes on the surface of hydrogels [24]. The Langmuir isotherm is represented by the following equation [40]:

$$\frac{C_e}{q_e} = \frac{1}{(q_{max} \cdot K_L)} + \frac{C_e}{q_{max}} \quad (3)$$

where q_e is the amount adsorbed, C_e the equilibrium concentration, q_{max} the maximum adsorption capacity reflected on a complete monolayer, and K_L represents the Langmuir constant that is related to the apparent energy of adsorption. A plot of C_e/q_e versus C_e should indicate a straight line of slope $(1/q_{max})$ and an intercept of $1/(K_L q_{max})$. The essential characteristics of the Langmuir isotherms can be described by a separation factor or equilibrium parameter (R_L), which is defined by the following equation [83]:

$$R_L = \frac{1}{1 + (K_L \cdot C_e)} \quad (4)$$

where R_L values indicate the type of adsorption to be irreversible ($R_L=0$), favorable ($0 < R_L < 1$), linear ($R_L=1$) or unfavorable ($R_L > 1$). This model is the most commonly used isothermal adsorption and has demonstrated good agreement with various experimental data [41][42]. The plots of the Langmuir adsorption isotherms of CR and BBY adsorbed on hydrogels AM, AMS, and AMSGO are shown in figure 6 (a and b), respectively, and table 2 presents the isothermal constants, q_{max} , K_L , R_L , and the correlation coefficient (R^2). As listed in table 2, the K_L offers information on the strength of adsorbate-adsorbent interaction. High the K_L value, the interaction is stronger and vice versa. In the present study, the K_L value for all prepared hydrogels was very small, this demonstrates that the interaction between these materials and dyes is weak [24]. Besides, Since the R_L value was found to be ($0 < R_L < 1$), the favorable isotherm has been confirmed and the R^2 was closed to unity, this confirmed that the Langmuir isotherm is applicable for the adsorption of dyes onto the prepared hydrogels [16] under the applied optimum conditions. While in the Freundlich model, which is based on adsorption on the surface of a heterogeneous multilayer, and assumes that the adsorption takes place at sites with varying energy of adsorption [43]. The Freundlich isotherm is represented as follow [44]:

$$\ln q_e = \ln K_F + \frac{1}{n} \ln C_e \quad (5)$$

where, K_F and $1/n$ are Freundlich constants related to adsorption capacity and adsorption intensity, respectively. K_F indicates the adsorption capacity of the adsorbent toward the adsorbate and the $1/n$ is an indicator for the degree of the surface heterogeneity which describes the distribution of the adsorbed molecules on the adsorbent surface. Overall, a value of n higher than 1 indicates that the adsorbate is favorably adsorbed on an adsorbent, and the higher the n value the stronger the adsorption intensity [43]. Illustrated in figure 7 (a and b), the fitting of Freundlich adsorption isotherm of CR, and BBY adsorbed onto prepared hydrogels and the intercept and slope of the plots of $\ln q_e$ against $\ln C_e$ were used to calculate the Freundlich isotherm constants K_F , $1/n$, and R^2 (Table 2). The value of $(1/n)$ indicates if the isotherm type is favorable for adsorption [16]. The adsorption process is favorable when the $1/n$ values are within the $0.1 < 1/n < 1$ range [45]. When the value of n is less than 1, the adsorption involves a chemical process. Otherwise, the adsorption is a physical mechanism [45][46]. In all of these studies, the values of $1/n$ for dyes were between 0.1 and 1 suggesting that the adsorption of both dyes favored chemisorption [45]. Typically, if the value of the correlation coefficient (R^2) approaches unity, the adsorption mechanism is said to obey a certain isotherm model i.e., the Langmuir or Freundlich isotherm

model [47]. Therefore, the dye adsorption by the synthesized hydrogels was consistent with the Langmuir isotherm model compare with that of the Freundlich isotherm, as indicated by the results shown in table 2.

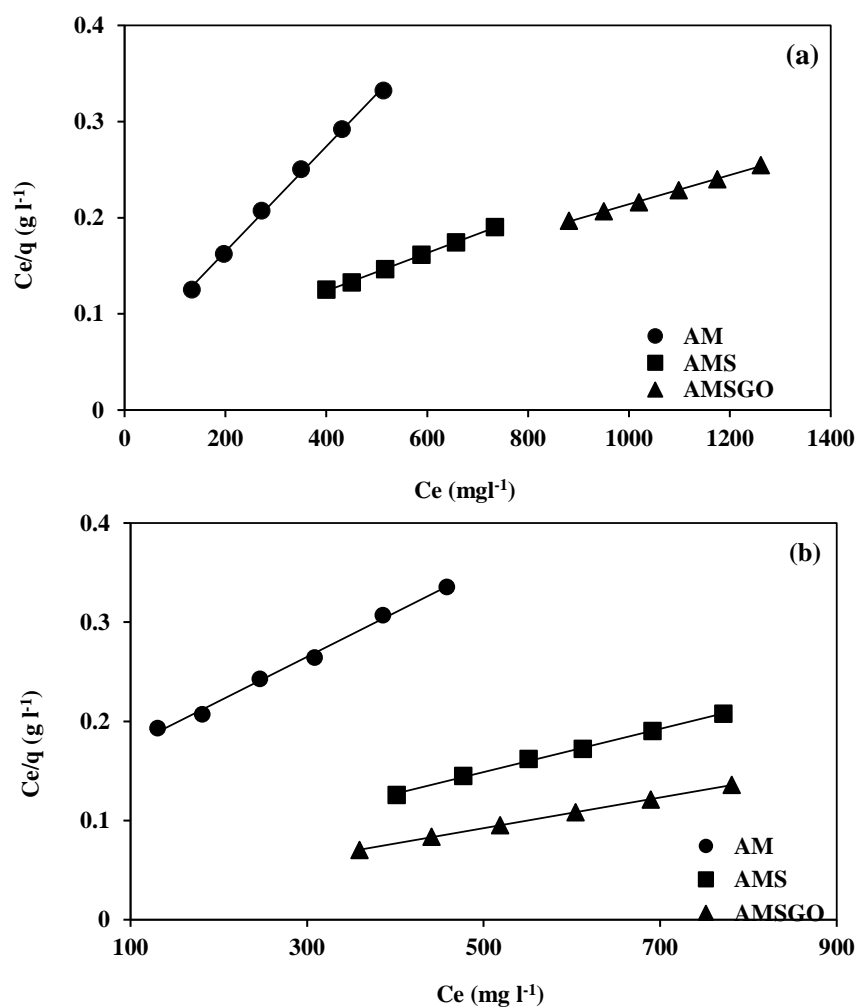


Figure 6. Langmuir adsorption of (a) CR and (b) BBY dyes onto AM, AMG, and AMGGO at 27 °C.

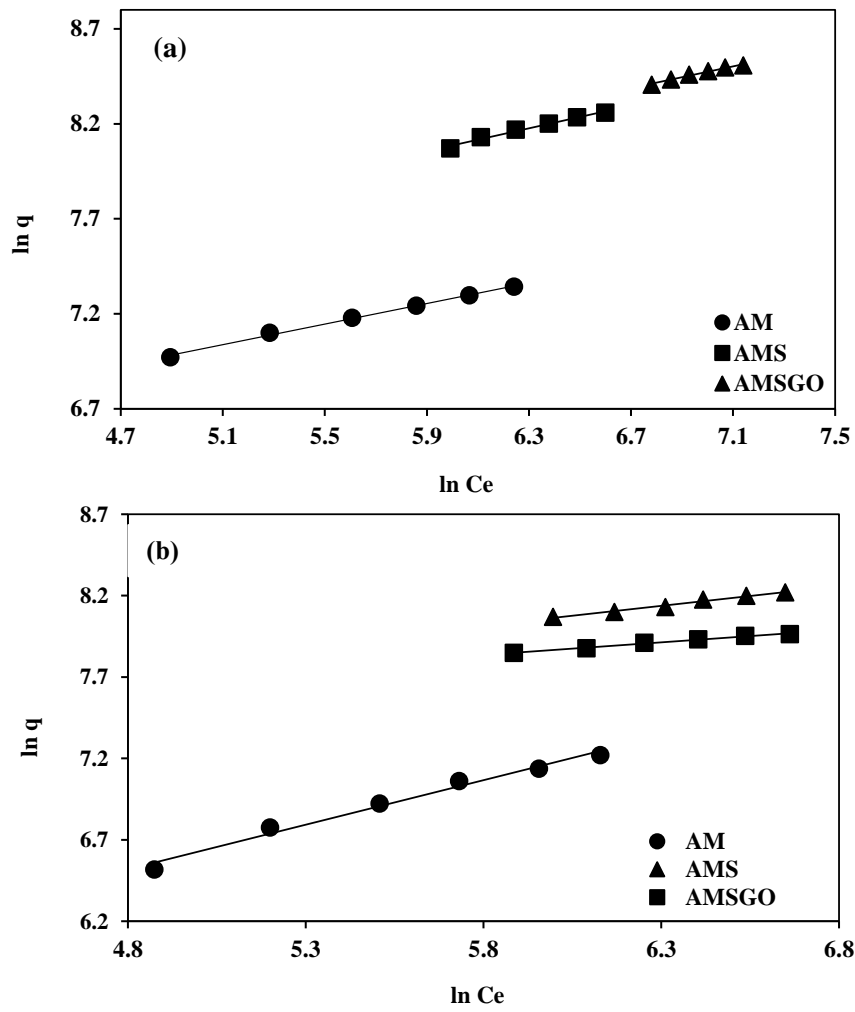


Figure 7. Freundlich adsorption of (a) CR and (b) BBY dyes onto AM, AMG, and AMGGO at 27 °C.

Table 2. Isotherm parameters for adsorption of dyes by hydrogels.

Samples	CR			BBY		
	AM	AMS	AMSGO	AM	AM	AMSGO
Langmuir						
q_{max} (mg g ⁻¹)	1830.16	5065.856	6600.66	2233.639	4587.156	6468.30
k_L	0.0098	0.00439	0.0024	0.0034	0.0055	0.0103
R_L	0.2027	0.1594	0.1712	0.4933	0.1322	0.0883
R^2	0.9984	0.9986	0.9986	0.9953	0.9977	0.9998
Freundlich						
K_F	286.179	538.56	650.956	49.088	741.400	1032.892
1/n	0.2708	0.2996	0.2851	0.5470	0.2427	0.1544
R^2	0.9967	0.98197	0.9841	0.9843	0.98499	0.9925

3.2.3. Kinetics of Dyes Adsorption

For a better understanding of the adsorption mechanism, the adsorption kinetic curves of the CR and BBY dyes onto prepared hydrogels were studied by kinetic models. In three kinetic models, including pseudo-first-order, pseudo-second-order, and intraparticle diffusion, experimental values were introduced, using the following equations [48]:

$$\ln(q_1 - q_t) = \ln q_1 - K_1 t \quad (6)$$

$$\frac{t}{q_t} = \frac{1}{K_2 q_2^2} + \left(\frac{1}{q_2}\right) t \quad (7)$$

$$q_t = k_p t^{1/2} + I \quad (8)$$

Where q_t , q_1 , and q_2 are the amounts of dye adsorbed by the prepared hydrogels at various time t , at equilibrium for the pseudo-first-order and pseudo-second-order, respectively. k_1 , k_2 , and k_p are the adsorption rate constants of the pseudo-first-order, pseudo-second-order, and intraparticle diffusion models. C is the intraparticle diffusion constant, which was related to the boundary layer thickness.

The experimental kinetic plots for the adsorption of CR and BBY dyes on prepared hydrogel are presented in figure 8-10 and figure 11-13, respectively. The kinetic parameters of kinetic models are summed up in tables 3 and 4: pseudo-first-order, pseudo-second-order, and intraparticle diffusion models. Good matching of the experimental data to the kinetic models was assessed by a high correlation coefficient (R^2) and close accord of the calculated and experimental (q_1 and q_2) values [30]. For all the prepared hydrogels, for CR and BBY dyes, the strong and pronounced disparity between the experimental absorption capacity and the calculated absorption capacity shows the deviation from pseudo-first-order kinetics. While the theoretical equilibrium adsorption capacities obtained from the pseudo-second-order model correlated well with the experimental results, with better correlation coefficients ($R^2 > 0.999$) values, thus indicating a well-fitting of the second-order model, compared to the pseudo-first-order kinetic model [49][50] Also, the adsorption rate k values were not always proportional to temperatures directly. The kinetic model of pseudo-second-order also notes that chemical adsorption is the rate-determining step. According to Eq. 8, if the key rate control step is intraparticle diffusion, the plot should be linear and pass through the origin. As illustrated in figures 10 and 13, the plots for CR and BBY dyes did not pass through the origin that suggests no intercept was found to be zero, which also implied that the diffusion intraparticle was not the only rate-determining step. From table 3 and 4, it is observed that values of k_p did not always directly proportional with temperatures. Values of constants C were nonzero and they increased in increasing temperature.

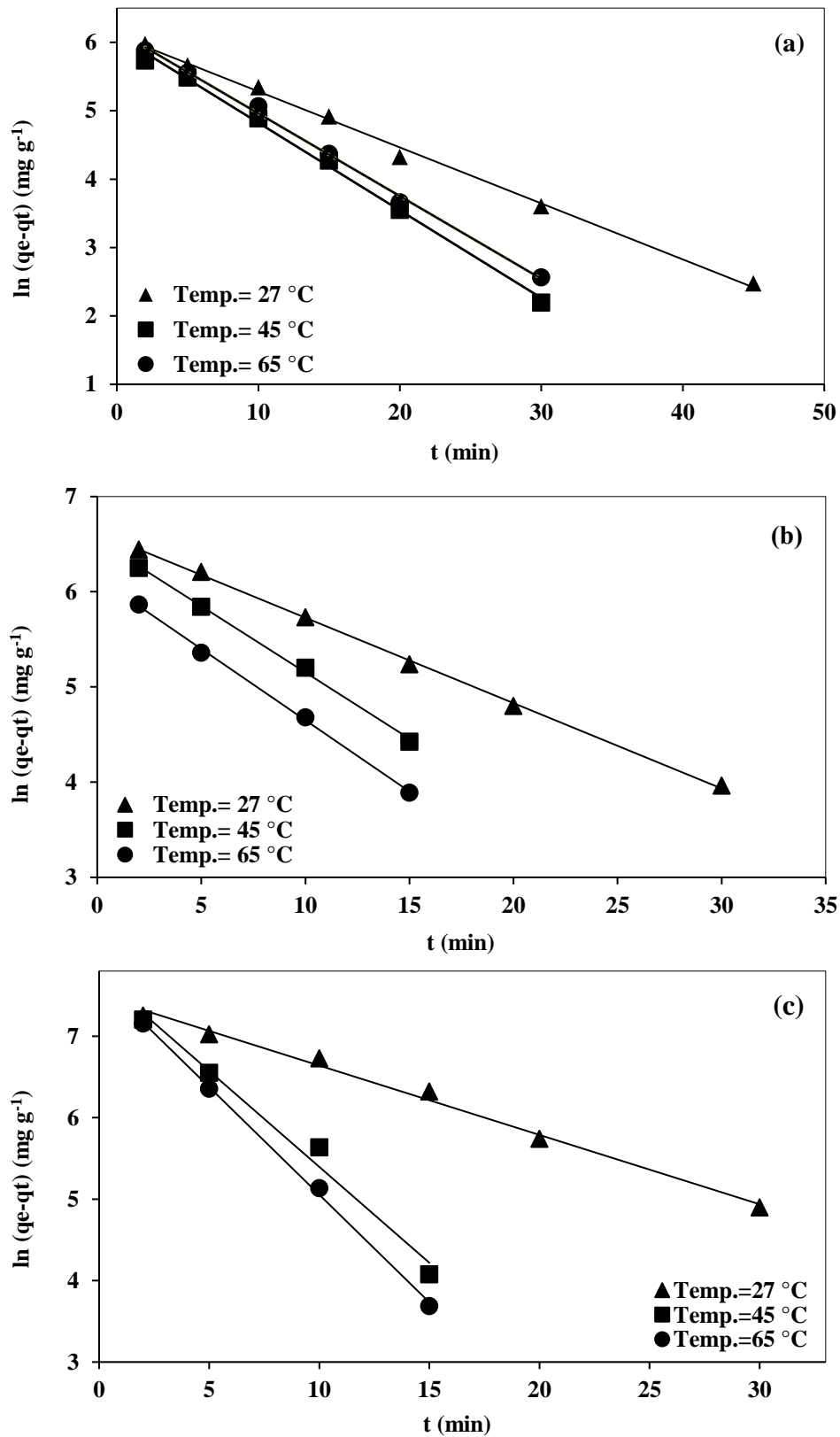


Figure 8. Pseudo-first order plot for the adsorption of CR dye onto (a) AM, (b) AMG, and (c) AMGGO at 27, 45, and 65 °C.

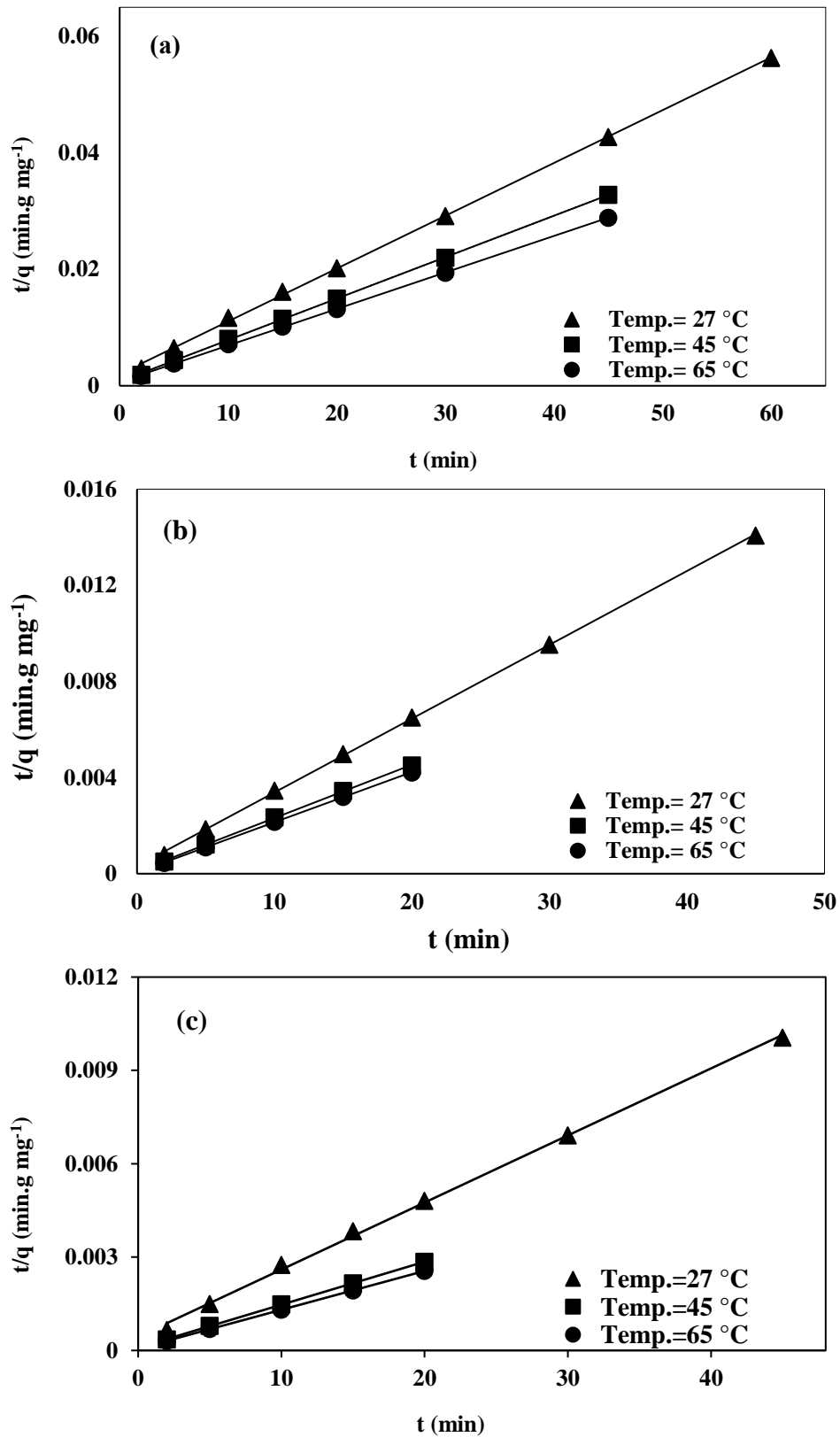


Figure 9. Pseudo-second order plot for the adsorption of CR dye onto (a) AM, (b) AMG, and (c) AMGGO at 27, 45, and 65 °C.

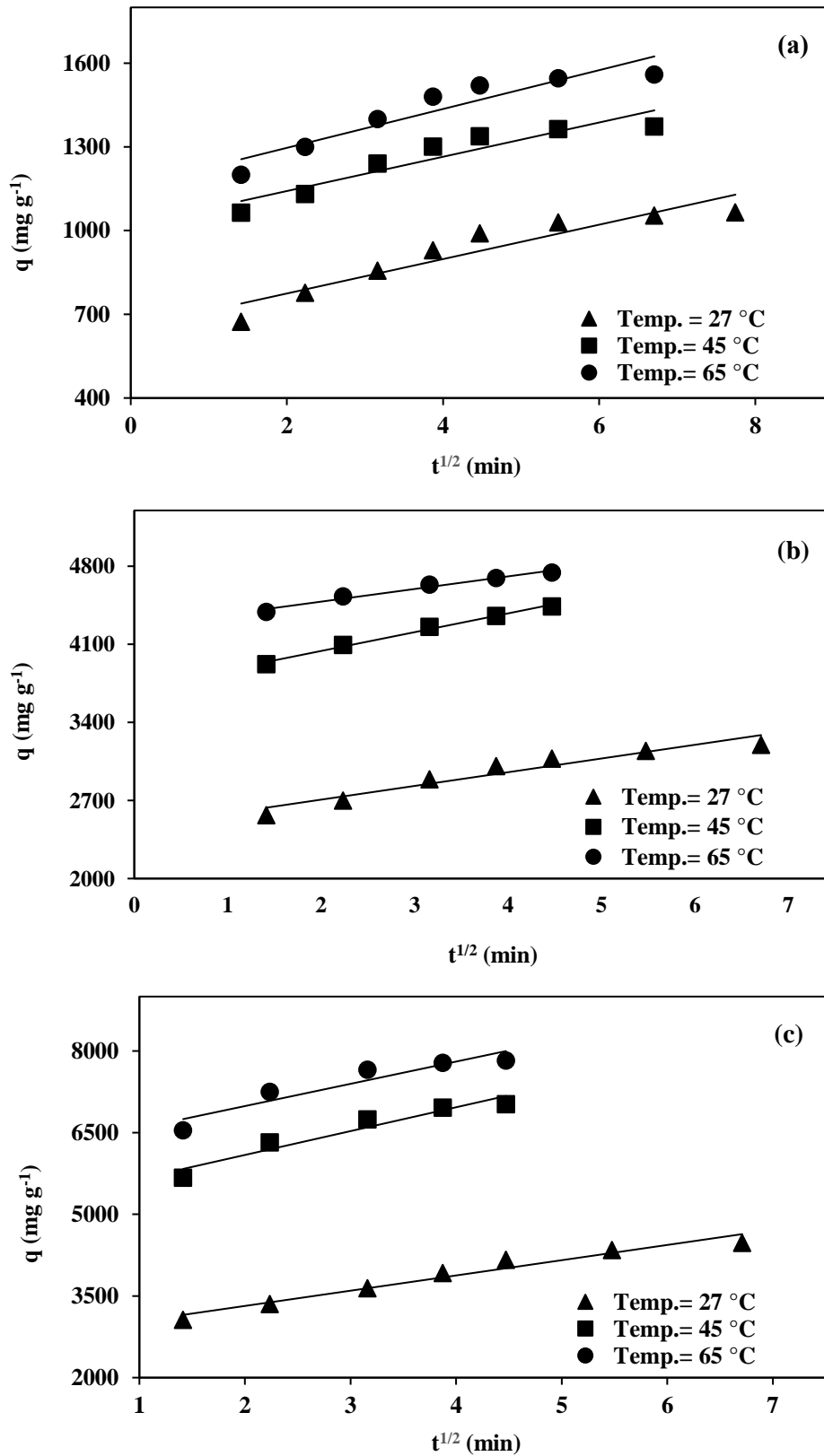


Figure 10. Intra-particle diffusion plot for the adsorption of CR dye onto (a) AM, (b) AMG, and (c) AMGGO at 27, 45, and 65 °C.

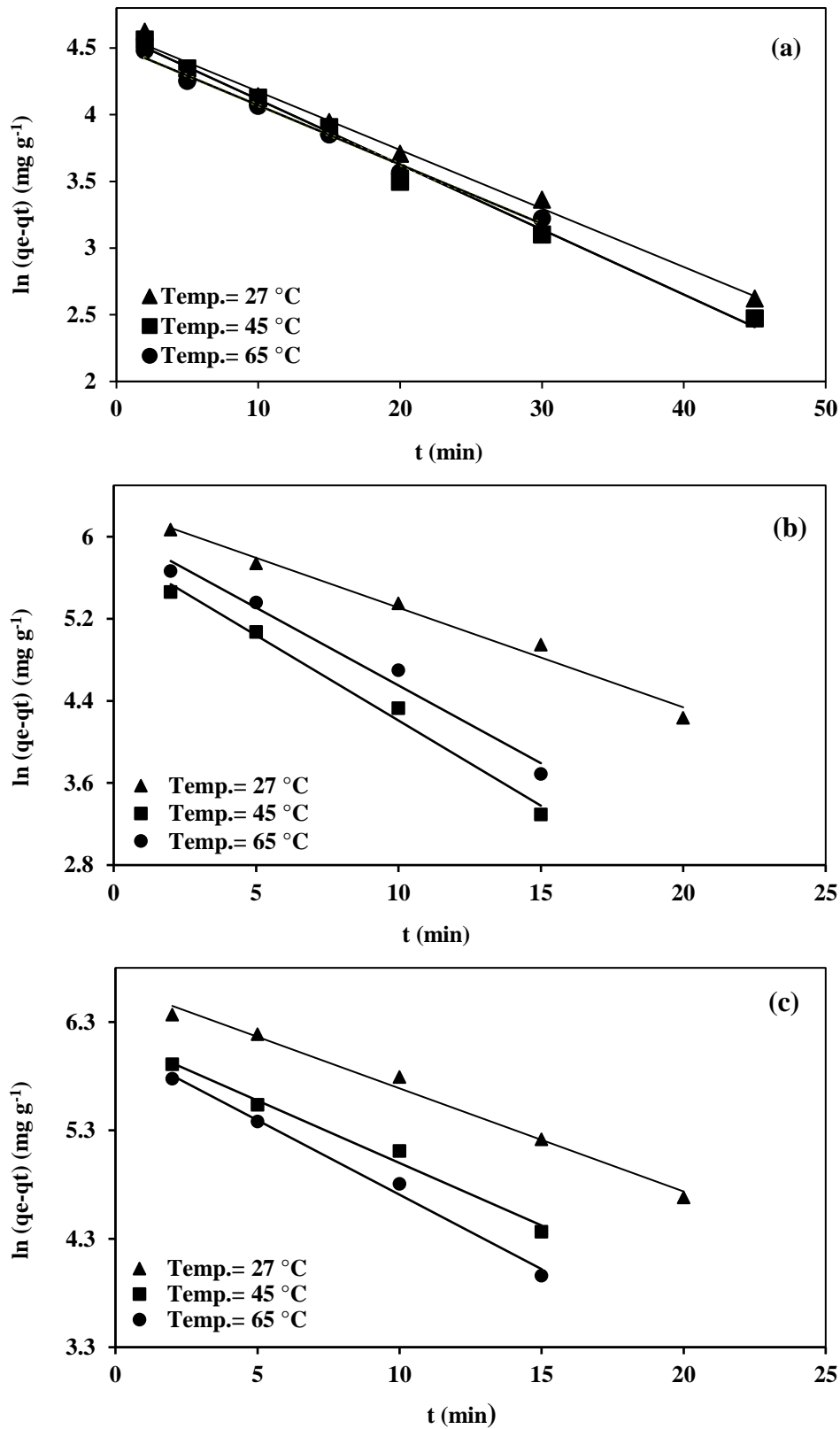


Figure 11. Pseudo-first order plot for the adsorption of BBY dye onto (a) AM, (b) AMG, and (c) AMGGO at 27, 45, and 65 °C.

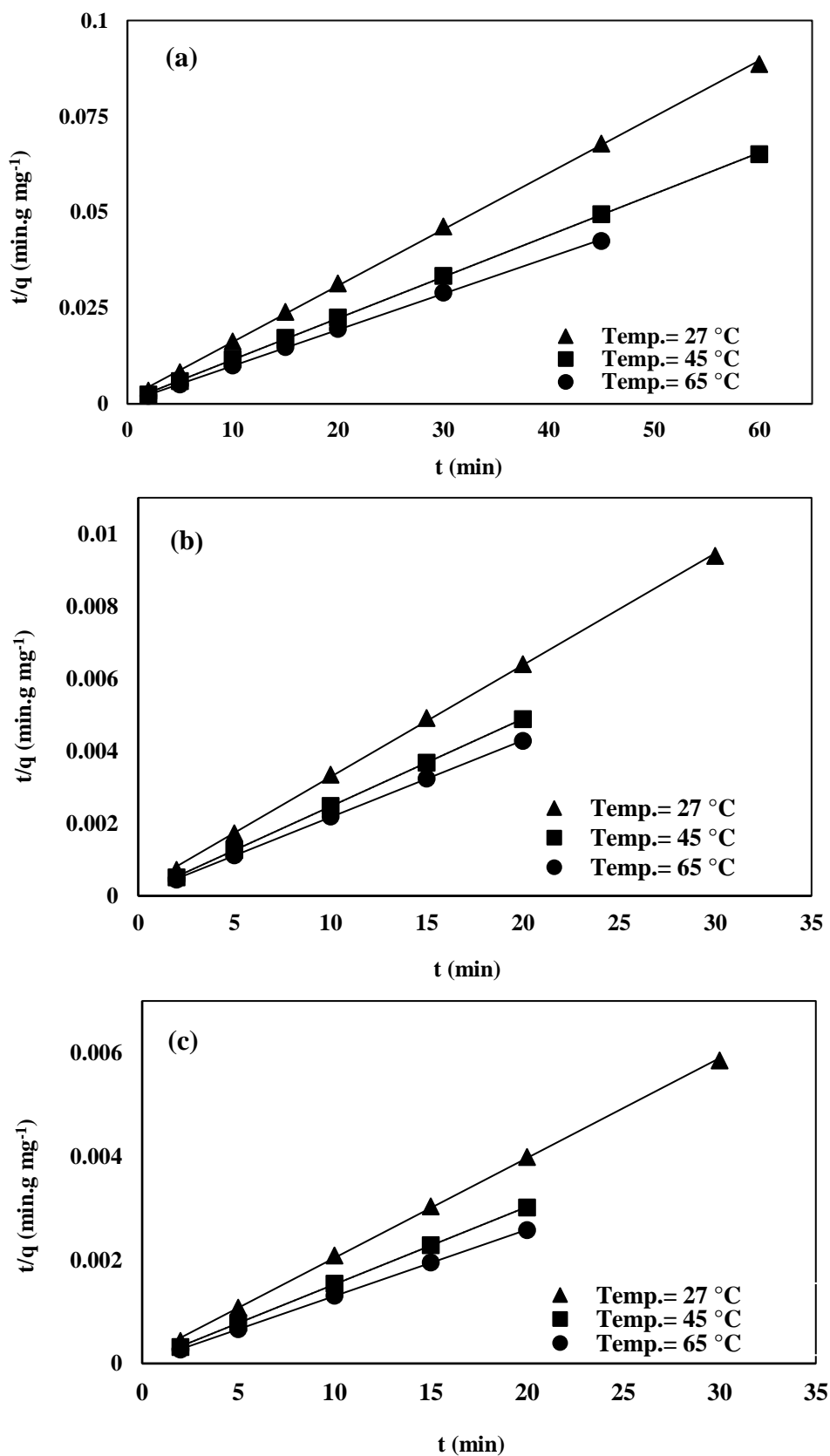


Figure 12. Pseudo-second order plot for the adsorption of BBY dye onto (a) AM, (b) AMG, and (c) AMGGO at 27, 45, and 65 °C.

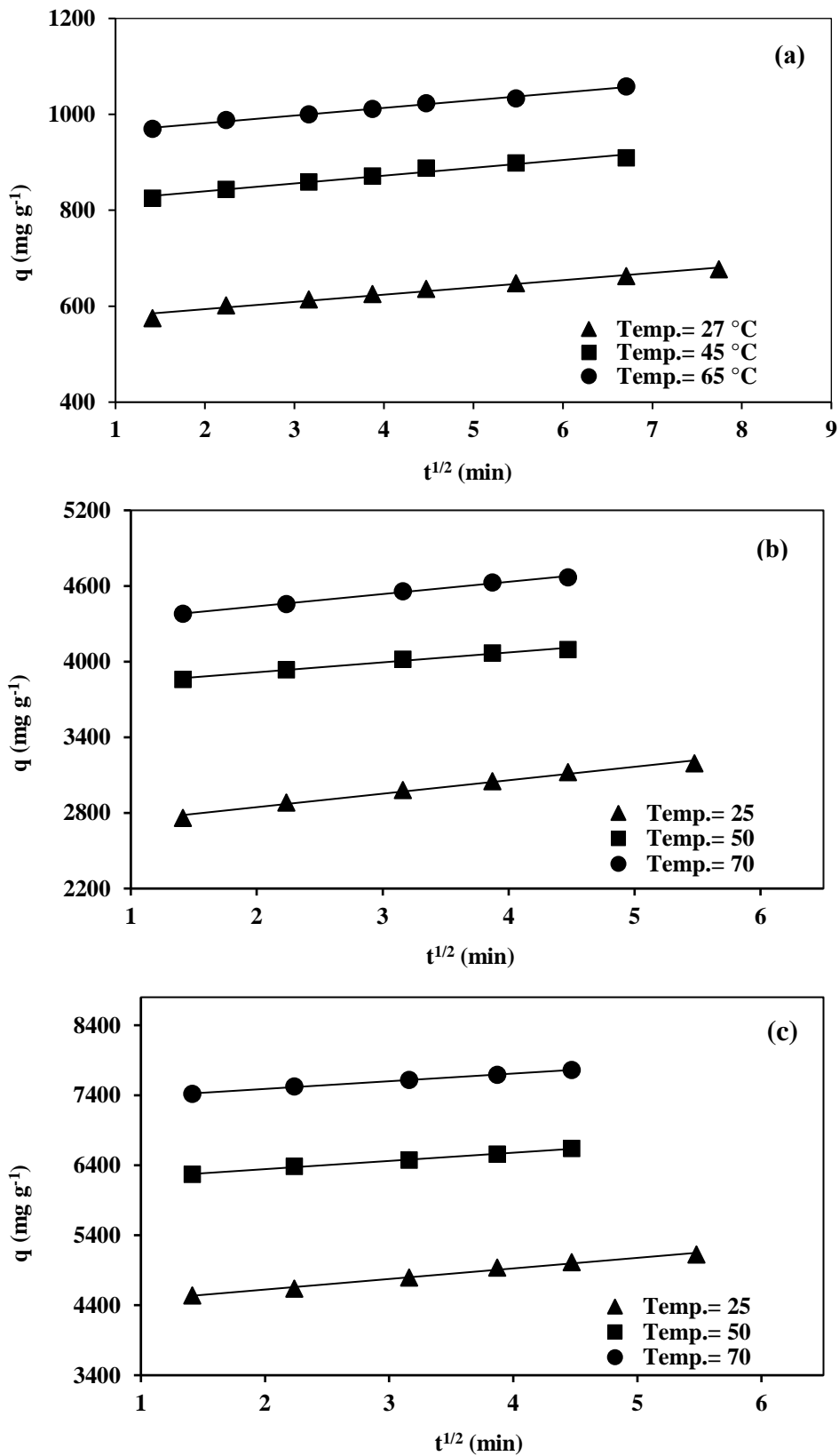


Figure 13. Intra-particle diffusion plot for the adsorption of BBY dye onto (a) AM, (b) AMG, and (c) AMGGO at 27, 45, and 65 °C.

Table 3. Kinetic parameters for adsorption of CR dye by the prepared hydrogels

T ($^{\circ}\text{C}$)	AM			AMS			AMSGO		
	27	45	65	27	45	65	27	45	65
q_{max} (Exp.) (mg g ⁻¹)	1065.7	1372.9	1559	3198.64	4440.13	4744.1	5123	6638.6	7762.5
Pseudo-first order									
q_1 (Cal.) (mg g ⁻¹)	446.35	447.85	478.02	753.51	695.95	468.22	764.45	469.64	437.33
K_1 (min ⁻¹)	0.0819	0.1280	0.1209	0.0897	0.1392	0.1498	0.0951	0.1153	0.1374
R_1^2	0.9965	0.99658	0.99715	0.9989	0.9979	0.9986	0.9891	0.9869	0.9921
Pseudo-second order									
q_2 (Cal.) (mg g ⁻¹)	1102.66	1404.89	1594.39	3256.27	4510.6	4789.27	5186.73	6680.03	7800.31
K_2 (g mg ⁻¹ min ⁻¹)	1.66E-09	3.78E-10	2.57E-10	2.93E-11	4.91E-12	2.34E-12	4.2E-12	7.28E-13	3.53E-13
R_2^2	0.9994	0.9998	0.9998	0.9997	0.9997	0.9999	0.9996	0.9999	0.9999
Intra-particle diffusion									
K_p	61.651	61.413	69.605	122.89	168.4	113.27	150.99	117.39	109.64
C	651.27	1018.9	1157.4	2461.8	3703.7	4256.1	4322.0	6109.4	7271.1
R_p^2	0.8889	0.8791	0.8783	0.9258	0.9922	0.9922	0.9897	0.9965	0.9979

Table 4. Kinetic parameters for adsorption of BBY dye by the prepared hydrogels

T ($^{\circ}\text{C}$)	AM			AMS			AMSGO		
	27	45	65	27	45	65	27	45	65
q_{max} (Exp.) (mg g ⁻¹)	676.76	921.02	1058.4	3193.1	4096	4669	4476	7020	7823
Pseudo-first order									
q_1 (Cal.) (mg g ⁻¹)	107.45	210.51	161.52	533.62	353.83	431.03	1792.65	2324.96	2202.75
K_1 (min ⁻¹)	0.0509	0.0470	0.0524	0.0971	0.1660	0.1516	0.0851	0.2355	0.2645
R_1^2	0.9864	0.9868	0.9641	0.9846	0.9897	0.9803	0.9925	0.98499	0.9987
Pseudo-second order									
q_2 (Cal.) (mg g ⁻¹)	681.06	925.84	1062.02	3237.29	4130.52	4710.32	4639.94	7243.23	8017.32
K_2 (g mg ⁻¹ min ⁻¹)	3.17E-09	8.41E-10	4.39E-10	1.9E-11	2.98E-12	2.33E-12	2.07E-11	1.73E-12	9.34E-13
R_2^2	0.9995	0.9998	0.9996	0.9995	0.9999	0.9999	0.9997	0.9997	0.9999
Intra-particle diffusion									
K_p	15.106	15.055	16.004	106.69	78.69	97.28	150.99	117.39	109.64
C	563.69	810.97	949.50	2631.9	3,757.7	4256.1	4322	6109.4	7271.1
R_p^2	0.9768	0.9701	0.9935	0.9872	0.9869	0.9956	0.9897	0.9965	0.9979

3.2.4. Thermodynamic of Dyes Adsorption

To specify whether prepared hydrogels adsorption is an endothermic or exothermic process, the thermodynamic investigation was carried out at various temperatures by calculating thermodynamic parameters namely, standard free energy (ΔG°), standard entropy change (ΔH°) and standard entropy change (ΔS°) using the following equations [51]:

$$K_L = \frac{C_a}{C_e} \quad (9)$$

$$\Delta G^\circ = -RT \ln K_L \quad (10)$$

$$\Delta G^\circ = \Delta H - T\Delta S^\circ \quad (11)$$

$$\ln K_L = \frac{\Delta S^\circ}{R} - \frac{\Delta H^\circ}{R} \frac{1}{T} \quad (12)$$

where K_L is the thermodynamic equilibrium constant, C_a and C_e are the equilibrium concentrations of CR, and BBY dyes on the hydrogel's adsorbents and in the solution, respectively. T is the absolute temperature, and R is the gas constant (8.314 J/molK). Thus, figures 14 (a and b) show the graphical representation of the obtained data by plotting $\ln K_L$ versus $1/T$. The graph's slope and intercept were used to calculate the ΔS° and ΔH° values and were tabled in table 5. The ΔG° could be calculated at different temperatures by equation (12) or (13).

Also, From the Arrhenius equation, the activation energy (E_a) that can be defined as the minimum amount of energy needed to proceed with the adsorption process was determined by using the following equation [51]:

$$\ln K = \ln A - \frac{E_a}{RT} \quad (13)$$

where K is the rate constant of the pseudo-second-order kinetic model for adsorption system of CR and BBY dyes since the adsorption analyzes are based on the constant obtained from linearized plots R^2 closest to unity, A is the Arrhenius factor, a straight line with a slope of $-E_a/R$ is obtained when $\ln K$ is graphed versus $1/T$, as shown in figure 15.

The calculated parameters for thermodynamics are shown in table 5. The positive value of ΔH° for the absorption process of CR and BBY dyes showed that the process was endothermic, which was supported by an increase in the absorption capacity of the prepared hydrogels. Similarly, the positive value of ΔS° for the adsorption of both dyes onto the prepared hydrogels suggests the high degree of randomness of the adsorption and affinity of the prepared hydrogels towards the dyes [11][52]. Also, the ΔG° values at all temperatures studied were negative, which underpins adsorption's spontaneous nature and indicates that the adsorption was thermodynamically favorable [53]. As seen in Table 6, with an increasing temperature of (300.15 - 338.15) K, the removal of CR and BBY dyes was less spontaneous. Nevertheless, the spontaneity of sample AM is lower compared to AMS and AMSGO [24]. In addition, the E_a data for the adsorption of CR and BBY dyes were obtained and indicated in table 5., which confirmed the dominant reaction is the chemisorption phenomenon. Also, it can be observed that the adsorption of both dyes onto AM have lower E_a values (less than 40 kJ/mol), this result suggested that the adsorption mechanism was physical adsorption, but the modification of AM could have alternated the adsorption mechanism to chemisorption with a higher E_a value [54].

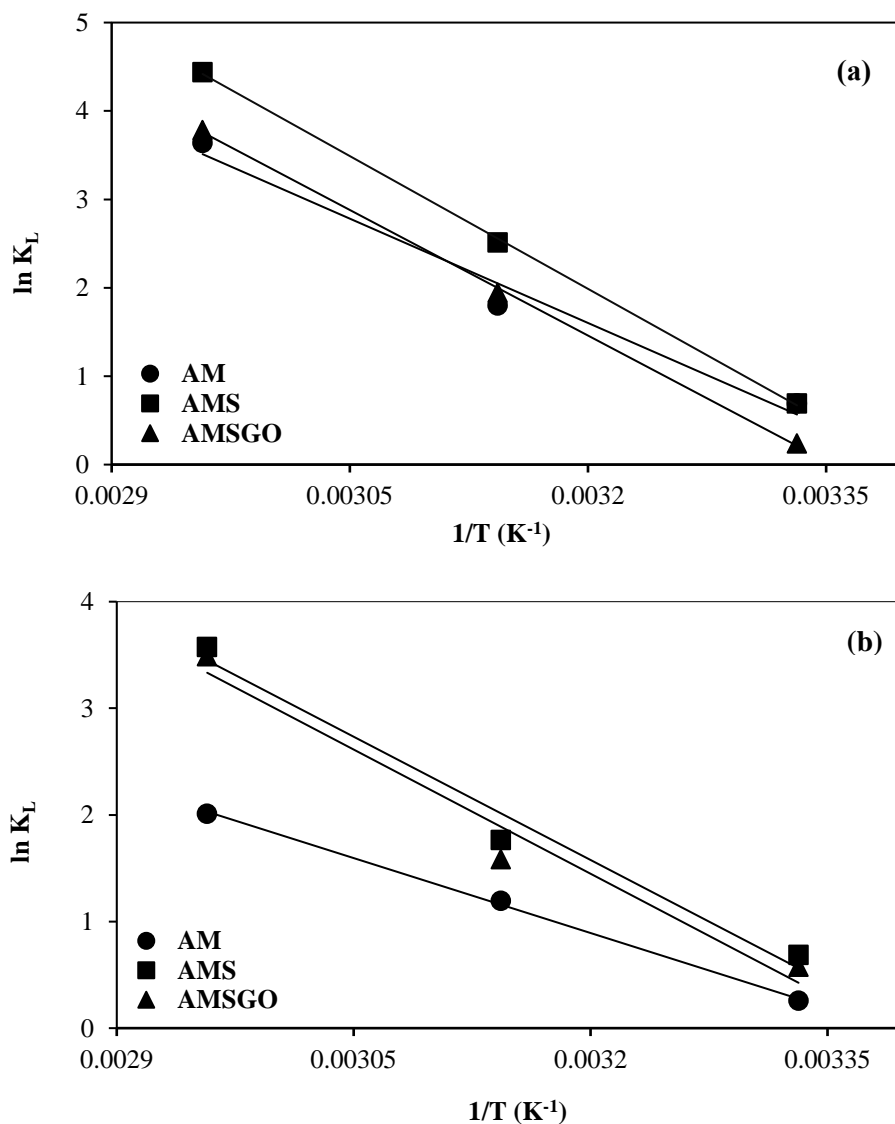


Figure 14. Plots of $\ln K_L$ vs. $1/T$ for estimation of thermodynamic parameters for the adsorption of (a) CR and (b) BBY dyes onto AM, AMG, and AMGGO

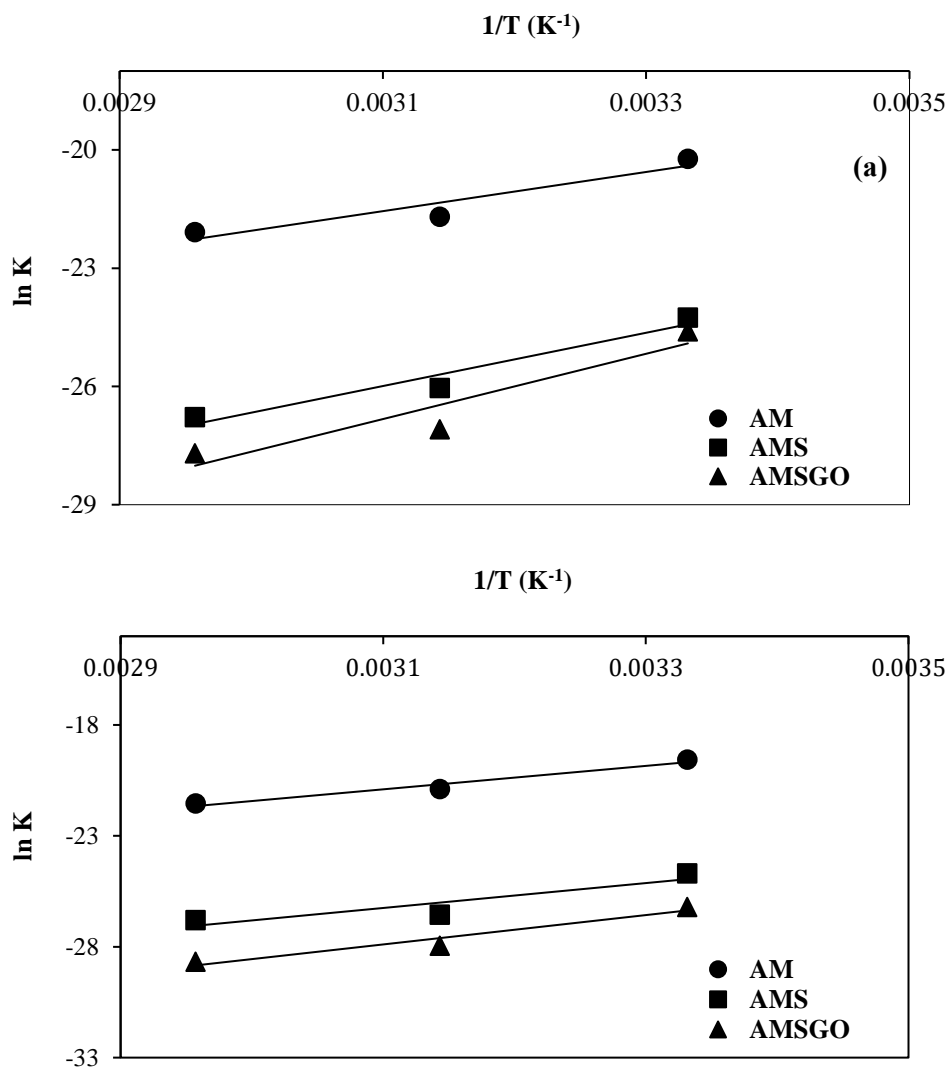


Figure 15. Plots of $\ln K$ vs. $1/T$ for estimation of activation energy for the adsorption of (a) CR and (b) BBY dyes onto AM, AMS, and AMSGO.

Table 5. Thermodynamic parameters for adsorption of CR and BBY dyes by the prepared hydrogels.

Temperature (K)	- ΔG° (KJ.mol ⁻¹)					
	CR			BBY		
	AM	AMS	AMSGO	AM	AMS	AMSGO
300.15	1.41	1.68	0.53	0.68	1.40	1.06
318.15	5.42	6.77	5.28	3.07	5.33	4.99
338.15	9.87	12.43	10.57	5.71	9.69	9.37
ΔH° (kJ.mol ⁻¹)	65.41	83.24	78.74	38.96	64.08	64.57
ΔS° (J.mol ⁻¹ .K ⁻¹)	222.63	282.91	264.09	132.09	218.18	218.66
Ea (KJ.mol ⁻¹)	39.90	56.19	68.87	37.75	46.67	55.00

3.3. Desorption Studies

Desorption studies are essential to understand the mechanism of adsorption [30]. Also, Adsorbent regeneration might improve the adsorption process more economically. Thus, successive desorption processes on the dyes used to evaluate the reusability of the prepared hydrogels over four consecutive cycles were carried out [55] and results are given in table 6, indicate that the percentage desorption was good for the four cycles. Therefore, the prepared hydrogels could be used repeatedly with retaining their good adsorption capacity.

Table 6: Adsorption-desorption for CR and BBY dye onto prepared hydrogels.

Cycles	CR						BBY					
	AM		AMS		AMSGO		AM		AMS		AMSGO	
	qe	%S	qe	%S	qe	%S	qe	%S	qe	%S	qe	%S
1	1080.2	95.5	3216.2	87.06	4482.7	80.210	679.6	94.15	3200.4	88.79	5136.6	81.64
2	960.3	90.8	3156.9	79.47	4407.2	71.34	663.5	90.43	3116.7	82.33	4918.9	74.45
3	823.5	82.2	3001.4	68.04	4200.3	60.47	612.5	84.68	2944.3	74.62	4566.3	65.93
4	608.1	75.6	2828.1	58.76	4012.4	48.93	559.6	76.49	2747.6	66.95	4232.6	54.89

References

- [1] H. Qadri, R. Ahmad, B. Mohammad, A. Mehmood, and G. Hamid, *Fresh Water Pollution Dynamics and Remediation*. 2020.
- [2] A. Inyinbor Adejumo, O. Adebisin Babatunde, P. Oluyori Abimbola, A. Adelani Akande Tabitha, O. Dada Adewumi, and A. Orefo Toyin, 'Water pollution: effects, prevention, and climatic impact', in *Water Challenges of an Urbanizing World*, vol. 33, IntechOpen: Rijeka, Croatia, 2018.
- [3] S. Ahmed and S. Ismail, 'Water pollution and its sources, effects and management: a case study of delhi', *Int. J. Curr. Adv. Res.*, 2018, 1, 2, 444.
- [4] Z. Li *et al.*, 'Adsorption of congo red and methylene blue dyes on an ashitaba waste and a walnut shell-based activated carbon from aqueous solutions: Experiments, characterization and physical interpretations', *Chem. Eng. J.*, 2020, 388, 124263.
- [5] H. Liu and H. Qiu, 'Recent advances of 3D graphene-based adsorbents for sample preparation of water pollutants: A review', *Chem. Eng. J.*, 2020, 393, 124691.
- [6] S. K. Ghosh, P. Das Saha, and M. F. Di, *Recent Trends in Waste Water Treatment and Water Resource Management*. Springer, 2020.

- [7] K. Z. Elwakeel, A. M. Elgarahy, G. A. Elshoubaky, and S. H. Mohammad, 'Microwave assist sorption of crystal violet and Congo red dyes onto amphoteric sorbent based on upcycled Sepia shells', *J. Environ. Heal. Sci. Eng.*, 2020, 18, 1, 35.
- [8] R. L. Kadam, Y. Kim, S. Gaikwad, M. Chang, N. H. Tarte, and S. Han, 'Catalytic decolorization of rhodamine B, Congo red, and crystal violet dyes, with a novel niobium oxide anchored molybdenum (Nb–O–Mo)', *Catalysts*, 2020, 10, 5.
- [9] V. K. Gupta, S. Agarwal, R. Ahmad, A. Mirza, and J. Mittal, 'Sequestration of toxic congo red dye from aqueous solution using ecofriendly guar gum/ activated carbon nanocomposite.', *Int. J. Biol. Macromol.*, 2020, 158, 1310.
- [10] A. Leudjo Taka, E. Fosso-Kankeu, K. Pillay, and X. Yangkou Mbianda, 'Metal nanoparticles decorated phosphorylated carbon nanotube/cyclodextrin nanosponge for trichloroethylene and Congo red dye adsorption from wastewater', *J. Environ. Chem. Eng.*, 2020, 8, 3, 103602, 2020.
- [11] A. A. Mizhir, A. A. Abdulwahid, and H. S. Al-Lami, 'Chemical functionalization graphene oxide for the adsorption behavior of bismarck brown dye from aqueous solutions', *Egyptian Journal of Chemistry*, 2020, 63, 5, 1679.
- [12] E. J. Mohammad, M. M. Kareem, and A. J. Atiyah, 'Removal of dye bismarck brown G by photocatalytic reaction over prepared co-oxide Cr₂O₃-NiO: A kinetic study', *Asian J. Chem.*, 2018, 30, 11, 2527.
- [13] J. L. Sousa and A. Aguiar, 'Influence of aromatic additives on Bismarck Brown Y dye color removal treatment by Fenton processes', *Environ. Sci. Pollut. Res.*, 2017, 24, 34, pp. 26734.
- [14] B. D. C. Ventura-camargo and M. A. Marin-morales, 'Azo Dyes: Characterization and Toxicity—A Review', *Text. Light Ind. Sci. Technol.*, 2013, 2, 2, 85.
- [15] A. Waheed, M. Mansha, I. W. Kazi, and N. Ullah, 'Synthesis of a novel 3,5-diacrylamidobenzoic acid based hyper-cross-linked resin for the efficient adsorption of Congo Red and Rhodamine B', *J. Hazard. Mater.*, 2019, 369, 528.
- [16] K. Kaur, R. Jindal, and D. Saini, 'Synthesis, optimization and characterization of PVA-co-poly(methacrylic acid) green adsorbents and applications in environmental remediation', *Polymer Bulletin*, 2020, 77, 6, 3079.
- [17] W. Wang *et al.*, 'High-performance two-dimensional montmorillonite supported-poly(acrylamide-co-acrylic acid) hydrogel for dye removal', *Environmental Pollution*, 2020, 257.
- [18] A. Verma *et al.*, 'Graphite modified sodium alginate hydrogel composite for efficient removal of malachite green dye', *Int. J. Biol. Macromol.*, 2020, 148, 1130.
- [19] T. U. Rehman, L. A. Shah, M. Khan, M. Irfan, and N. S. Khattak, 'Zwitterionic superabsorbent polymer hydrogels for efficient and selective removal of organic dyes', *RSC Adv.*, 2019, 9, 32, 18565.
- [20] A. M. Atta, A. K. Gafer, H. A. Al-Lohedan, M. Abdullah, A. M. Tawfeek, and A. O. Ezzat, 'Hybrid Ionic Silver and Magnetite Microgels Nanocomposites for Efficient Removal of Methylene Blue', *Molecules*, 2019, 24, 21, 3867.
- [21] F. Bibi, M. Ajmal, F. Naseer, Z. H. Farooqi, and M. Siddiq, 'Preparation of magnetic microgels for catalytic reduction of 4-nitrophenol and removal of methylene blue from aqueous medium', *Int. J. Environ. Sci. Technol.*, 2018, 15, 4, 863.
- [22] A. Pourjavadi, M. Nazari, B. Kabiri, S. H. Hosseini, and C. Bennett, 'Preparation of porous graphene oxide/hydrogel nanocomposites and their ability for efficient adsorption of methylene blue', *RSC Adv.*, 2016, 6, 13, 10430.
- [23] R. Bera, A. Dey, and D. Chakrabarty, 'Tuning of the swelling and dye removal efficacy of poly(acrylamide-AMPS)-based smart hydrogel', *Sep. Sci. Technol.*, 2016, 52, 4, 743.
- [24] T. U. Rehman *et al.*, 'Fabrication of stable superabsorbent hydrogels for successful removal of crystal violet from waste water', *RSC Adv.*, 2019, 9, 68, 40051.
- [25] S. Scalese *et al.*, 'Cationic and anionic azo-dye removal from water by sulfonated graphene oxide nanosheets in Nafion nanocomposite membranes', 2016.

- [26] J. Y. C. Lim, S. S. Goh, S. S. Liow, K. Xue, and X. J. Loh, 'Molecular gel sorbent materials for environmental remediation and wastewater treatment', *J. Mater. Chem. A*, 2019, 7, 32, 18759.
- [27] A. O. da Silva *et al.*, 'Effect of graphene oxide coating on the ballistic performance of aramid fabric', *J. Mater. Res. Technol.*, 2020, v9, 2, 2267.
- [28] E. Yilmaz, G. Guzel Kaya, and H. Deveci, 'Removal of methylene blue dye from aqueous solution by semi-interpenetrating polymer network hybrid hydrogel: Optimization through Taguchi method', *J. Polym. Sci. Part A Polym. Chem.*, 2019, 57, 10, 1070.
- [29] S. Mohebbi, D. Bastani, and H. Shayesteh, 'Equilibrium, kinetic and thermodynamic studies of a low-cost biosorbent for the removal of Congo red dye: acid and CTAB-acid modified celery (*Apium graveolens*)', *J. Mol. Struct.*, 2019, 1176, 181.
- [30] L. Soldatkina and M. Zavrichko, 'Equilibrium, kinetic, and thermodynamic studies of anionic dyes adsorption on corn stalks modified by cetylpyridinium bromide', *Colloids and Interfaces*, 2019, 3, 1, 4.
- [31] J. Li, X. Zeng, T. Ren, and E. van der Heide, 'The preparation of graphene oxide and its derivatives and their application in bio-tribological systems', *Lubricants*, 2014, 2, 3, 137.
- [32] L. Zhu, Y. Liu, F. Wang, T. He, Y. Tang, and J. Yang, 'Preparation and the swelling properties of sodium alginate graft poly (acrylic acid-co-2-acrylamide-2-methyl propane sulfonic acid)/graphene oxide hydrogel composite', *Adv. Polym. Technol.*, 2018, 37, 8, 2885.
- [33] M. Zhong, Y.-T. Liu, and X.-M. Xie, 'Self-healable, super tough graphene oxide-poly (acrylic acid) nanocomposite hydrogels facilitated by dual cross-linking effects through dynamic ionic interactions', *J. Mater. Chem. B*, 2015, 3, 19, 4001.
- [34] M. A. Awad and L. S. Jasim Al-Hayder, 'Removal of a Boprolol drug from Aqueous Solutions onto Graphene Oxide/Carboymethyl cellulose sodium / Acryl acid polymer Composite by Adsorption', *IOP Conf. Ser. Mater. Sci. Eng.*, 2020, 928, 5.
- [35] M. A. Al-Ghouti and R. S. Al-Absi, 'Mechanistic understanding of the adsorption and thermodynamic aspects of cationic methylene blue dye onto cellulosic olive stones biomass from wastewater', *Sci. Rep.*, 2020, 10, 1, 1–18.
- [36] N. Ayawei, A. N. Ebelegi, and D. Wankasi, 'Modelling and interpretation of adsorption isotherms', *J. Chem.*, 2017, 2017.
- [37] C. Shih, J. Park, D. S. Sholl, M. J. Realff, T. Yajima, and Y. Kawajiri, 'Hierarchical Bayesian estimation for adsorption isotherm parameter determination', *Chem. Eng. Sci.*, 2020, 214, 115435.
- [38] B. Dash, B. Dash, and S. S. Rath, 'A thorough understanding of the adsorption of Ni (II), Cd (II) and Zn (II) on goethite using experiments and molecular dynamics simulation', *Sep. Purif. Technol.*, 2020, 240, 116649.
- [39] J. Wu, A. Xia, C. Chen, L. Feng, X. Su, and X. Wang, 'Adsorption thermodynamics and dynamics of three typical dyes onto bio-adsorbent spent substrate of *Pleurotus eryngii*', *Int. J. Environ. Res. Public Health*, 2019, 16, 5, 679.
- [40] I. Langmuir, 'The adsorption of gases on plane surfaces of glass, mica and platinum.', *J. Am. Chem. Soc.*, 1918, 40, 9, 1361.
- [41] K. Y. Foo and B. H. Hameed, 'Insights into the modeling of adsorption isotherm systems', *Chem. Eng. J.*, 2010, 156, 1, 2–10.
- [42] A. H. Sulaymon, T. J. Mohammed, and J. Al-Najar, 'Equilibrium and kinetics studies of adsorption of heavy metals onto activated carbon', *Can. J. Chem. Eng. Technol.*, 2012, 3, 4, 86.
- [43] C. M. Hussain, *Nanomaterials in chromatography: current trends in chromatographic research technology and techniques*. Elsevier, 2018.
- [44] H. Freundlich, 'The uptake of substances on solid surfaces', *Physicse Chem. Soc.*, 1906, 40, pp. 1361.
- [45] S. Saber-Samandari, H. O. Gulcan, S. Saber-Samandari, and M. Gazi, 'Efficient removal of anionic and cationic dyes from an aqueous solution using pullulan-graft-polyacrylamide porous hydrogel', *Water. Air. Soil Pollut.*, 2014, 225, 11.

- [46] A. O. Ifelebuegu, 'Removal of steroid hormones by activated carbon adsorption—kinetic and thermodynamic studies', *J. Environ. Prot. (Irvine, Calif.)*, 2012, 3, 6, 469.
- [47] K. Bello, B. K. Sarojini, and B. Narayana, 'Design and fabrication of environmentally benign cellulose based hydrogel matrix for selective adsorption of toxic dyes from industrial effluvia', *J. Polym. Res.*, 2019, 26, 3, 1.
- [48] F. A. Ugbe and N. Abdus-Salam, 'Kinetics and thermodynamic modelling of natural and synthetic goethite for dyes scavenging from aqueous systems', *Arab. J. Chem. Environ. Res.*, 2020, 7, 1, 12.
- [49] J. T. Utsev, R. T. Iwar, and K. J. Ifyalem, 'Adsorption of methylene blue from aqueous solution onto delonix regia pod activated carbon: batch equilibrium isotherm, kinetic and thermodynamic studies', *Agric. wastes*, 2020, 4, 5, 18.
- [50] S. Ahmadi and F. K. Mostafapour, 'Adsorptive removal of aniline from aqueous solutions by Pistacia atlantica (Baneh) shells: isotherm and kinetic studies', *J Sci Technol Env. Inf.*, 2017, 5, 1, 327.
- [51] M. Erdem, E. Yüksel, T. Tay, Y. Çimen, and H. Türk, 'Synthesis of novel methacrylate based adsorbents and their sorptive properties towards p-nitrophenol from aqueous solutions', *J. Colloid Interface Sci.*, 2009, 333, 1, 40.
- [52] A. A. Abdulwahid *et al.*, 'An efficient reusable perylene hydrogel for removing some toxic dyes from contaminated water', *Polym. Int.*
- [53] A. Murcia-Salvador *et al.*, 'Adsorption of Direct Blue 78 using chitosan and cyclodextrins as adsorbents', *Polymers (Basel)*, 2019, 11 6, 1003.
- [54] S. Chakraborty, A. Mukherjee, S. Das, N. R. Maddela, S. Iram, and P. Das, 'Study on isotherm, kinetics, and thermodynamics of adsorption of crystal violet dye by calcium oxide modified fly ash', *Environ. Eng. Res.*, 2021, 26, 1, 1.
- [55] W. T. Al-Rubayee, O. F. Abdul-Rasheed, and N. M. Ali, 'Preparation of a Modified Nanoalumina Sorbent for the Removal of Alizarin Yellow R and Methylene Blue Dyes from Aqueous Solutions', *J. Chem.*, 2016, 2016.